BMC Cancer

RESEARCH Open Access

Down-regulated HHLA2 enhances neoadjuvant immunotherapy efficacy in patients with non-small cell lung cancer (NSCLC) with chronic obstructive pulmonary disease (COPD)

Ao Zeng[1†], Yanze Yin[1†], Zhilong Xu[1], Abudumijiti Abuduwayiti[1], Fujun Yang[1], Mohammed Saud Shaik[2], Chao Wang[1], Keyi Chen[1], Chao Wang[1], Xinyun Fang[1] and Jie Dai[1*]

Abstract

Background Emerging data suggested a favorable outcome in advanced non-small cell lung cancer (NSCLC) with chronic obstructive pulmonary disease (COPD) patients treated by immunotherapy. The objective of this study was to investigate the effectiveness of neoadjuvant immunotherapy among NSCLC with COPD versus NSCLC without COPD and explore the potential mechanistic links.

Patients and methods Patients with NSCLC receiving neoadjuvant immunotherapy and surgery at Shanghai Pulmonary Hospital between November 2020 and January 2023 were reviewed. The assessment of neoadjuvant immunotherapy's effectiveness was conducted based on the major pathologic response (MPR). The gene expression profile was investigated by RNA sequencing data. Immune cell proportions were examined using flow cytometry. The association between gene expression, immune cells, and pathologic response was validated by immunohistochemistry and single-cell data.

Results A total of 230 NSCLC patients who received neoadjuvant immunotherapy were analyzed, including 60 (26.1%) with COPD. Multivariate logistic regression demonstrated that COPD was a predictor for MPR after neoadjuvant immunotherapy [odds ratio (OR), 2.490; 95% confidence interval (CI), 1.295–4.912; $P=0.007$]. NSCLC with COPD showed a down-regulation of HERV–H LTR-associating protein 2 (HHLA2), which was an immune checkpoint molecule, and the HHLA2^{low} group demonstrated the enrichment of CD8^{+}CD103^{+} tissue-resident memory T cells (TRM) compared to the HHLA2^{high} group (11.9% vs. 4.2%, $P=0.013$). Single-cell analysis revealed TRM enrichment in

†Ao Zeng and Yanze Yin contributed equally to this work and share first authorship.

*Correspondence:
Jie Dai
daijie@tongji.edu.cn

Full list of author information is available at the end of the article

the MPR group. Similarly, NSCLC with COPD exhibited a higher proportion of $CD8^+CD103^+$TRM compared to NSCLC without COPD (11.9% vs. 4.6%, $P=0.040$).

Conclusions The study identified NSCLC with COPD as a favorable lung cancer type for neoadjuvant immunotherapy, offering a new perspective on the multimodality treatment of this patient population. Down-regulated HHLA2 in NSCLC with COPD might improve the MPR rate to neoadjuvant immunotherapy owing to the enrichment of $CD8^+CD103^+$TRM.

Trial registration Approval for the collection and utilization of clinical samples was granted by the Ethics Committee of Shanghai Pulmonary Hospital (Approval number: K23-228).

Keywords Non-small cell lung cancer, Chronic obstructive pulmonary disease, Neoadjuvant immunotherapy, HERV–H LTR-associating protein 2, Tissue-resident memory T cells

Introduction

Lung cancer is a highly prevalent and deadly disease. Previous research has shown that the incidence rate of non-small cell lung cancer (NSCLC) patients with chronic obstructive pulmonary disease (COPD) could reach as high as 50.5%[1]. NSCLC with COPD was reported to have a worse survival prognosis compared to NSCLC without COPD [2]. Immune checkpoint inhibitors (ICI) have become a viable strategy in cancer therapy; however, The rate of response was merely 12.5% in unselected patients [3]. Programmed cell death ligand 1 (PD-L1), tumor mutational burden (TMB), and mismatch repair (MMR)–deficient/microsatellite instability were reported to predict immunotherapy efficacy [4]. Zhou et al. found that NSCLC with COPD patients with advanced stage receiving anti-programmed cell death 1 (PD1)/PD-L1 immunotherapy obtained a more prolonged progression-free survival (PFS) in contrast to NSCLC without COPD patients [5]. In addition, emphysema, a typical manifestation of COPD, was also associated with an improved response to immunotherapy in NSCLC patients [6–8]. Nevertheless, additional research is required to determine whether NSCLC with COPD patients continue to represent a predominant population that benefits from neoadjuvant immunotherapy.

HERV–H LTR-associating protein 2 (HHLA2), alternatively identified as B7-H7, was a recently unveiled addition to the B7 family considered an immune checkpoint [9]. HHLA2 exhibited broad expression in human malignancies, including lung and breast cancer. Given its immunosuppressive function, HHLA2 was identified as a promising target for human cancer immunotherapy [10]. Previous research demonstrated that HHLA2 exhibited primary expression on both tumor cell and antigen-presenting cell (APC) membranes [9–12], inhibiting human $CD4^+$ and $CD8^+$T cell proliferation and activation when T cell receptor signaling was present [9, 13, 14]. However, the specific role of HHLA2 in NSCLC with COPD treated by immunotherapy has not yet been elucidated.

Tissue-resident memory T cells (TRM) constituted a specific $CD8^+$ memory T cell subset, known to generate a potent anti-tumor immune response, and were linked to improved patient outcomes [15]. TRM were characterized by their presence within the tissue and exhibited enrichment of immune checkpoints and cytotoxic molecules, suggesting their significant contribution to tumor immunity [16]. Furthermore, the accumulation of $CD8^+CD103^+$TRM within tumors was a promising indicator for forecasting the effectiveness of ICI [17]. Nevertheless, the specific role of $CD8^+CD103^+$TRM in the response of NSCLC with COPD to immunotherapy remains unclear.

The objective of this study was to investigate the effectiveness of neoadjuvant immunotherapy among NSCLC with COPD versus NSCLC without COPD, and further explored the potential mechanistic links.

Patients and methods

Clinical data collection

Four hundred twenty lung cancer patients who underwent neoadjuvant immunotherapy in Shanghai Pulmonary Hospital from November 2020 to January 2023 were included. The inclusion criteria comprised the followings: (I) diagnosed with NSCLC; (II) with precise postoperative pathologic response degree. The exclusion criteria consisted of the followings: (I) incomplete neoadjuvant immunotherapy information; (II) a history of other malignancies; (III) without pre-neoadjuvant immunotherapy pulmonary function. Ultimately, 230 NSCLC patients were encompassed. Clinical and pathologic data were collected for all patients. Major pathologic response (MPR) was characterized by the presence of residual viable tumor not exceeding 10% at the time of resection. The diagnosis of COPD was based on forced expiratory volume in one second (FEV1)/forced vital capacity (FVC) < 0.70.

Clinical samples collection

The clinical samples used for HE staining, immunohistochemistry, and flow cytometry were obtained from Shanghai Pulmonary Hospital with the patient's informed consent. Approval for the collection and utilization of

clinical samples was granted by the Ethics Committee of Shanghai Pulmonary Hospital (Ethical approval number: K23-228).

RNA sequencing data

Forty NSCLC fresh-frozen specimens from our cohort were subjected to RNA sequencing analysis. The samples were processed to extract total RNA to assess its quality. RNA was further quantified and amplified. Subsequently, amplified RNA was fragmented and processed. Raw RNA sequencing data were further scanned. Additionally, RNA sequencing data of 1041 NSCLC tissues were obtained from The Cancer Genome Atlas (TCGA) database, including 175 samples with post-bronchodilator pulmonary function. Differential gene analysis was conducted using the Deseq2 package in the R software (https://www.r-project.org/) for both our cohort and the 175 TCGA samples data. Genes with an absolute value of $Log_2FC>2$ and P value<0.05 were regarded as differentially expressed. The volcanic map was generated using the online platform (https://www.bioinformatics.com.cn), last accessed on 20 Feb 2023, to visualize the differential gene. The Venn diagram was plotted using Venny2.1.0 (https://bioinfogp.cnb.csic.es/tools/venny/index.html) to identify overlapping differential genes.

Immunologic gene sets from the MSigDB database (https://www.gsea-msigdb.org/gsea/msigdb/) and the immunologic infiltration analysis were analyzed using TCGA RNA sequencing data [18].

Single-cell sequencing analysis

Single-cell data of patients receiving neoadjuvant immunotherapy from the Gene Expression Omnibus (GEO) dataset (GSE173351) were collected and analyzed [19]. After quality control, 42,678 T cells were remained for further analysis, and 15 distinct cell clusters were identified.

HE staining

Paraffin-embedded slices of NSCLC samples were prepared and processed through dewaxing, dehydration, hematoxylin, and eosin staining. After dehydration, the slices were sealed with neutral gum. The extent of tumor cell necrosis was evaluated and recorded using an optical microscope. Based on the ratio of the tumor necrotic area to the entire area, we have divided it into four score grades as follows: score 1: 0-25%; score 2: 26-50%; score 3: 51-75%; score 4: 76-100%.

Immunohistochemistry

Paraffin-embedded NSCLC samples underwent dewaxing and hydration. 3% H_2O_2 was used to block endogenous peroxidase activity. Antigen retrieval was conducted through microwave heating in a citrate buffer. The slices were incubated overnight with an anti-HHLA2 antibody. Subsequently, a secondary antibody labeled with horseradish peroxidase (HRP) was applied. The visualization of HHLA2 expression was achieved through DAB color rendering, and nuclear restaining was performed. The staining intensity for HHLA2 was evaluated to determine its expression in cells, and quantitative protein analysis was carried out using Image J software.

Immunofluorescence

Paraffin slices were dewaxed and dehydrated, followed by antigen retrieval using citrate buffers. The slices were sealed with serum and double stained with primary antibodies against CD8 and CD103. Species-specific secondary antibodies labeled with HRP were applied, followed by DAPI nuclear restaining. Microscopic observation and quantitative cell analysis using Image J software were performed.

Flow cytometry

Tumor samples were immediately minced and digested using collagenase IV in a 37℃ water bath. To achieve a single-cell suspension, the cell suspension obtained was filtered using a 70 μm filter. The single-cell suspension was processed through gradient centrifugation using a Percoll lymphocyte isolation solution to separate immune cells. The isolated immune cells were further lysed to remove red blood cells and stored at -80℃ for later use. For flow cytometry analysis, the cells were subsequently stained with fluorescent-labeled antibodies against live/dead (APCCY7), CD3 (BV510), CD4 (BB700), CD8 (BV605), CD103 (FITC), PD1 (APC), granzyme B (GZMB) (BV421), and interferon gamma (IFNG) (PE). The stained cells were then examined through the CytoFLEX system, and the acquired data were analyzed with FlowJo V10.6.2 software.

Statistical analysis

Statistical analyses were performed utilizing R software and GraphPad Prism9. Logistic regression analysis was used to investigate the determinants of neoadjuvant immunotherapy efficacy. The rates between the two groups were compared using either the Chi-square test or Fisher's exact test. Student's t-test was used to analyze normally distributed continuous variables, while non-normally distributed continuous variables were assessed employing a nonparametric test. The statistical significance threshold was set at $P<0.05$, and all analyses were performed using a two-tailed approach.

Results

NSCLC with COPD patients obtained a higher MPR rate to neoadjuvant immunotherapy

This study encompassed 230 NSCLC patients who underwent neoadjuvant immunotherapy. The median age was 64 years old [interquartile range (IQR), 58.0–68.0], with the majority of patients being male (n=214, 93.0%) and smokers (n=179, 77.8%). There were 60 (26.1%) NSCLC with COPD patients. NSCLC with COPD exhibited similar gender (P=0.077), age (P=0.072), and PD-L1 expression levels (P=0.748) as NSCLC without COPD patients (Table 1).

Table 1 Basic information of NSCLC without COPD and NSCLC with COPD patients

Characteristics	Total	NSCLC without COPD	NSCLC with COPD	P
	n=230	n=170	n=60	
Gender				0.077
Male	214 (93.0)	155 (91.2)	59 (98.3)	
Female	16 (7.0)	15 (8.8)	1 (1.7)	
Age	64.0 [58.0;68.0]	64.0 [58.0;68.0]	65.0 [60.0;69.0]	0.072
Pathology				0.058
LUAD	59 (25.7)	49 (28.8)	10 (16.7)	
LUSC	135 (58.7)	92 (54.1)	43 (71.7)	
Others	36 (15.6)	29 (17.1)	7 (11.6)	
Neoadjuvant regimen				0.346
Immunotherapy only	1 (0.5)	1 (0.6)	0 (0.0)	
Immuno + Chemotherapy	214 (93.0)	157 (92.4)	57 (95.0)	
Immuno + Targeted/ Anti-vascular therapy	8 (3.5)	5 (2.9)	3 (5.0)	
Immuno + Chemo + Targeted therapy	7 (3.0)	7 (4.1)	0 (0.0)	
Pathologic response				0.004
Non-MPR	110 (47.8)	91 (53.5)	19 (31.7)	
MPR	120 (52.2)	79 (46.5)	41 (68.3)	
Clinical stage				0.044
I/II	65 (28.3)	42 (24.7)	23 (38.3)	
III	165 (71.7)	128 (75.3)	37 (61.7)	
Treatment cycles	3.0 [2.0;4.0]	3.0 [2.0;4.0]	3.0 [2.0;4.0]	0.778
Smoking history				0.227
No	15 (6.5)	14 (8.2)	1 (1.7)	
Yes	179 (77.8)	129 (75.9)	50 (83.3)	
Unknown	36 (15.7)	27 (15.9)	9 (15.0)	
FEV1	2.4 [1.9;2.8]	2.5 [2.2;2.9]	1.9 [1.6;2.2]	<0.001
FEV1%	87.7 [74.3;98.1]	92.1 [83.3;102.0]	67.3 [56.2;75.6]	<0.001
PD-L1 expression				0.748
PD-L1 < 50%	123 (53.5)	93 (54.7)	30 (50.0)	
PD-L1 ≥ 50%	29 (12.6)	20 (11.8)	9 (15.0)	
Unknown	78 (33.9)	57 (33.5)	21 (35.0)	

Values are presented as median [IQR1-IQR3] or n (%); IQR, interquartile range; NSCLC, non-small cell lung cancer; MPR, major pathologic response; LUSC, lung squamous cell carcinoma; LUAD, lung adenocarcinoma; COPD, chronic obstructive pulmonary disease; FEV1, forced expiratory volume in one second; PD-L1, programmed cell death ligand 1

In addition, pathologic results showed that 120 (52.2%) patients achieved MPR following neoadjuvant immunotherapy. There were no noteworthy disparities in the MPR rates between different age groups and clinical stages in NSCLC patients. NSCLC with COPD had a higher MPR rate to neoadjuvant immunotherapy compared to NSCLC without COPD (68.3% vs. 46.5%, P=0.004). Additionally, patients with a smoking history, higher PD-L1 expression or lung squamous cell carcinoma (LUSC) responded better to immunotherapy (Table 2; Fig. 1A).

Univariate analysis showed that COPD exhibited a significant association with MPR [odds ratio (OR), 2.486; 95% confidence interval (CI), 1.350–4.708; P=0.004], along with pathology, PD-L1 expression and gender. Multivariate logistic regression analysis confirmed that COPD remained as an predictor associated with a better response to neoadjuvant immunotherapy (OR, 2.490; 95%CI, 1.295–4.912; P=0.007) (Table 2). Furthermore, HE staining of pathologic specimens revealed more pronounced tumor cell necrosis in NSCLC with COPD (Fig. 1B-C).

NSCLC with COPD showed a down-regulation of HHLA2

Differential gene analysis was conducted using RNA sequencing data of 40 samples from our cohort, including NSCLC with COPD (n=12) and NSCLC without COPD (n=28). 226 differential genes were detected, comprising 142 down-regulated and 84 up-regulated genes (Fig. 2A). Differential gene analysis was also performed using RNA sequencing data from 175 TCGA samples with post-bronchodilator pulmonary function, including NSCLC with COPD (n=65) and NSCLC without COPD (n=110). Seventy differential genes were found, including 53 down-regulated and 17 up-regulated genes (Fig. 2A). By comparing the two datasets, we discovered ten down-regulated (HHLA2, BRINP1, CA10, CEACAM8, CLDN6, HNF4A, LGALS4, OLFM4, SERPINA4 and UGT2B15) and one up-regulated (S100A7) genes that were consistently differentially expressed (Fig. 2B). And then, the down-regulated HHLA2 was selected for further investigation due to its relevance to tumor immunity. Immunohistochemical staining of tissue slices confirmed that HHLA2 expression was lower in NSCLC with COPD (n=20) compared to NSCLC without COPD (n=42) (Fig. 2C-D). In addition, immunohistochemical staining showed that HHLA2 expression was also lower in the MPR group (Fig. 2E-F).

Table 2 Factors affecting neoadjuvant immunotherapy efficacy of NSCLC patients

Characteristics	*n* = 230	MPR 120 (52.2)	Univariate			Multivariate		
			OR	95%CI	P	OR	95%CI	P
Gender								
Male	214	116 (54.2)	reference			reference		
Female	16	4 (25.0)	0.282	0.077–0.837	0.033	0.273	0.062–0.981	0.059
Age								
Age ≤ 60	77	39 (50.7)	reference					
Age > 60	153	81 (53.0)	1.096	0.633–1.898	0.743			
Pathology								
LUSC	135	71 (52.6)	reference			reference		
LUAD	59	22 (37.3)	0.536	0.283–0.996	0.051	0.690	0.340–1.384	0.298
Others	36	27 (75.0)	2.704	1.222–6.487	0.018	3.478	1.484–8.842	0.006
Clinical stage								
III	165	85 (51.5)	reference					
I/II	65	35 (53.8)	1.098	0.618–1.959	0.750			
Treatment cycles								
Cycles < 4	156	87 (55.8)	reference					
Cycles ≥ 4	74	33 (44.6)	0.664	0.378–1.158	0.150			
Smoking history								
Yes	179	95 (53.1)	reference					
No	15	4 (26.7)	0.322	0.087–0.980	0.060			
Unknown	36	21 (58.3)	1.238	0.603–2.594	0.564			
COPD								
No	170	79 (46.5)	reference			reference		
Yes	60	41 (68.3)	2.486	1.350–4.708	0.004	2.490	1.295–4.912	0.007
PD-L1 expression								
PD-L1 < 50%	123	57 (46.3)	reference			reference		
PD-L1 ≥ 50%	29	23 (79.3)	4.439	1.785–12.703	0.002	5.235	1.976–16.045	0.002
Unknown	78	40 (51.3)	1.219	0.691–2.156	0.495	1.229	0.661–2.293	0.515

Values are presented as n (%); NSCLC, non-small cell lung cancer; MPR, major pathologic response; OR, odds ratio; CI, confidence interval; LUSC, lung squamous cell carcinoma; LUAD, lung adenocarcinoma; COPD, chronic obstructive pulmonary disease; PD-L1, programmed cell death ligand 1

Down-regulated HHLA2 was associated with CD8$^+$CD103$^+$TRM enrichment

TCGA RNA sequencing data of 1041 samples were analyzed and categorized into HHLA2^{high} (n=520) and HHLA2^{low} (n=521) groups according to the median expression level of HHLA2. Using the MSigDB database to perform immune function scoring on the two groups, the HHLA2^{high} group exhibited higher scores in gene sets related to inhibiting immune response, T cell proliferation, and CD8$^+$T cell activation than the HHLA2^{low} group (Fig. 3A). These results suggested that HHLA2 may be linked to the tumor microenvironment.

To explore the correlation between HHLA2 and the tumor microenvironment, 19 samples assessed for HHLA2 expression via immunohistochemistry were further divided into two groups: HHLA2^{high} (n=10) and HHLA2^{low} (n=9) based on median HHLA2 expression for the flow cytometry analysis. The flow cytometry analysis showed that a greater proportion of CD8$^+$CD103$^+$TRM within CD3$^+$ cells was observed in the HHLA2^{low} group compared to the HHLA2^{high} group (11.9% vs. 4.2%, P=0.013). However, there were no statistically significant differences in the expression levels of GZMB, IFNG, and PD1 in CD8$^+$CD103$^+$TRM between the two groups (Fig. 3B-D). These findings demonstrated that down-regulated HHLA2 was associated with CD8$^+$CD103$^+$TRM enrichment in the tumor microenvironment.

Enrichment of CD8$^+$CD103$^+$TRM in the MPR group

Single-cell data from six NSCLC patients, including the MPR (n=3) and non-MPR group (n=3), were analyzed. The study identified 42,678 T cells and 15 distinct cell clusters, including CD8$^+$ effector T cells (GZMK, NKG7), stress response state T cells (T-STR) defined by the elevated expression of heat shock genes (HSPA1A, HSPA1B) [20], CD8$^+$ proliferating T cells (TUBB, STMN1), stem-like memory T cells (CCR7, IL7R), CD4$^+$ T follicular helper cells (Tfh) (KLRB1, NR3C1), CD4$^+$ regulatory T cells (Treg) (FOXP3, IL2RA), CD8$^+$TRM (CD8A, ITGAE known as CD103), and CD8$^+$ exhausted T cells (CD8A, PDCD1) (Fig. 4A-B). Among all the T cells, 1181 cells were identified as CD8$^+$CD103$^+$TRM. The MPR group comprised 20,271

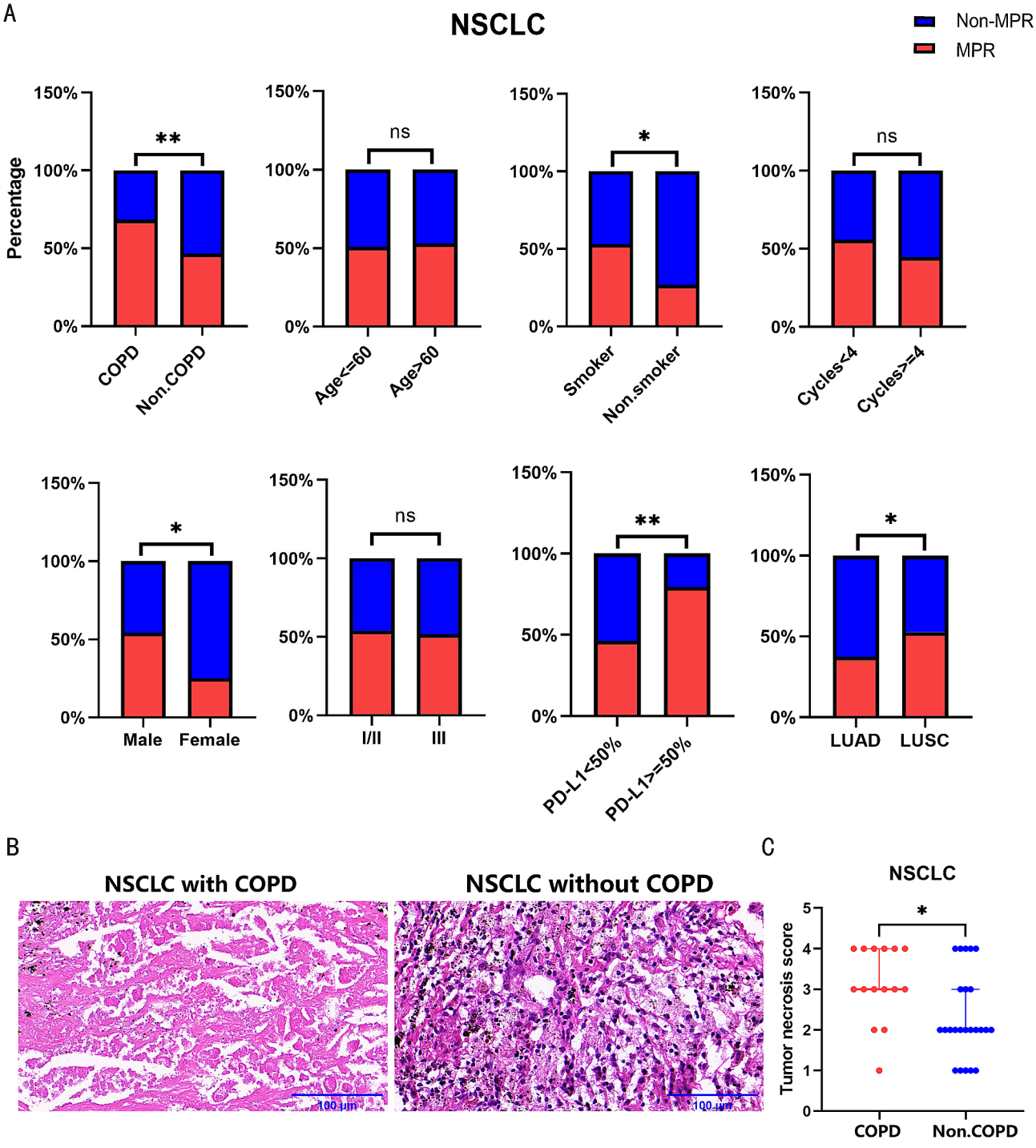

Fig. 1 NSCLC with COPD patients obtained a higher MPR rate to neoadjuvant immunotherapy. (**A**) The efficacy to neoadjuvant immunotherapy in NSCLC patients with different COPD status, age, smoking history, gender, clinical stage, PD-L1 expression, treatment cycles, and pathology were compared. (**B**) Representative pictures of HE staining of patients received neoadjuvant immunotherapy. Left: NSCLC with COPD; Right: NSCLC without COPD. (**C**) Statistical chart of HE staining in NSCLC with COPD versus NSCLC without COPD patients received neoadjuvant immunotherapy. Scale bars, 100 μm.*$P < 0.05$, **$P < 0.01$, ***$P < 0.001$, ****$P < 0.0001$

single cells, including 614 $CD8^+CD103^+$TRM, while the non-MPR group comprised 22,407 single cells, with 567 $CD8^+CD103^+$TRM (Fig. 4C). Notably, a higher proportion of $CD8^+CD103^+$TRM was observed in the MPR group in contrast to the non-MPR group (3.0% vs. 2.5%, $P=0.002$) (Fig. 4D). Differences of additional typical cell clusters between the MPR and non-MPR groups were shown in supplementary Figure S1. Immunofluorescence

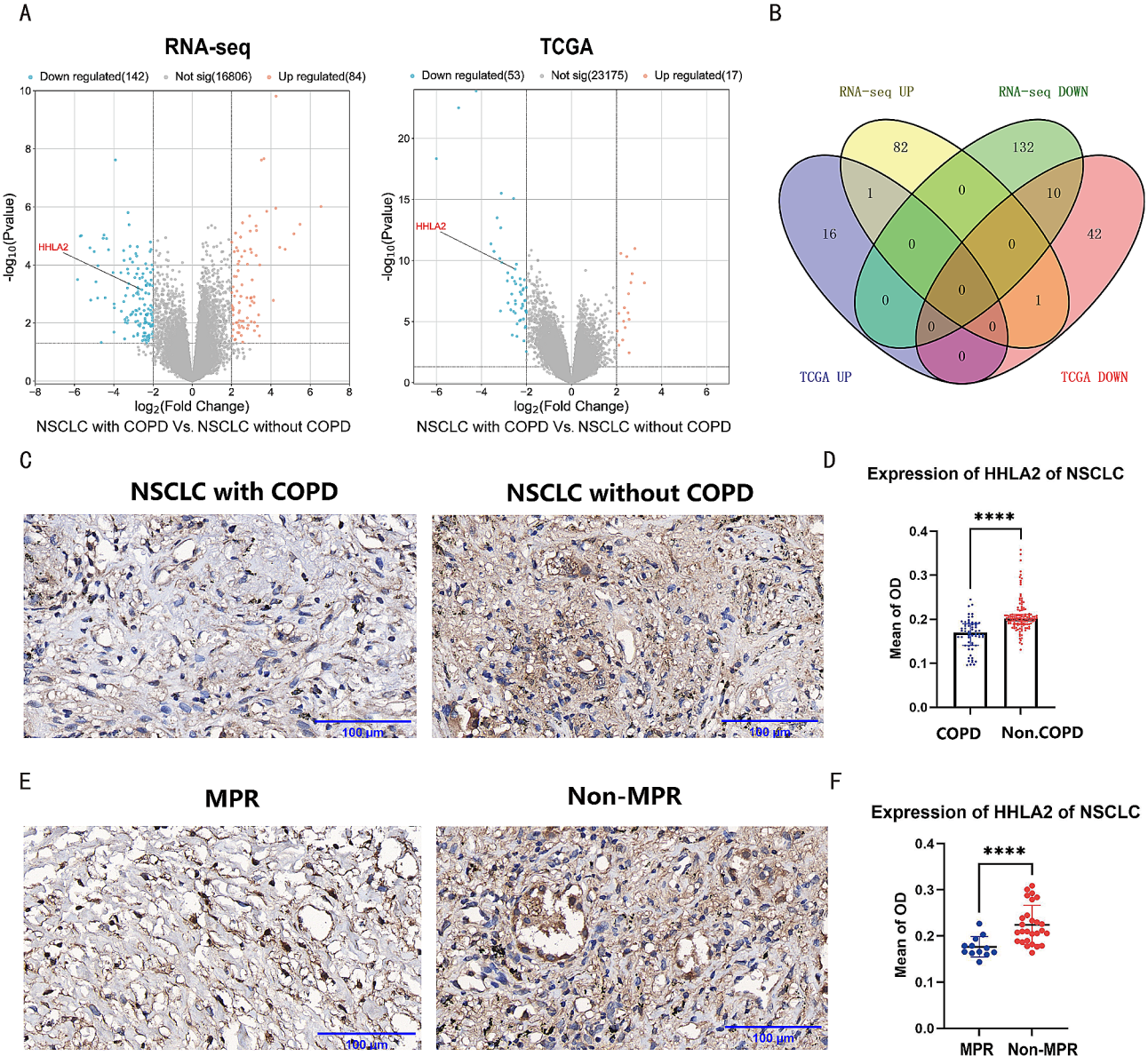

Fig. 2 NSCLC with COPD showed a down-regulation of HHLA2. (**A**) Left: Volcanic map of differential genes in 40 samples paired with NSCLC with COPD and NSCLC without COPD. Right: Volcanic map of differential genes in 175 TCGA samples paired with NSCLC with COPD and NSCLC without COPD. The blue and orange dots represent down-regulated and up-regulated genes, respectively. (**B**) Venn diagram of the intersection of differential genes mentioned above. (**C**) Representative image of HHLA2 immunohistochemical staining. Left: NSCLC with COPD; Right: NSCLC without COPD. (**D**) Statistical chart of HHLA2 immunohistochemical staining in NSCLC with COPD versus NSCLC without COPD. (**E**) Representative images of HHLA2 immunohistochemical staining. Left: the MPR group; Right: the non-MPR group. (**F**) Statistical chart of HHLA2 immunohistochemical staining in the MPR group versus the non-MPR group. Scale bars, 100 μm. *$P<0.05$, **$P<0.01$, ***$P<0.001$, ****$P<0.0001$

analysis further demonstrated the enrichment of TRM in the MPR group as opposed to the non-MPR group (Fig. 4E-F). These results implied that the enrichment of TRM was correlated with MPR.

NSCLC with COPD was featured by $CD8^+CD103^+$TRM enrichment

RNA sequencing data of 175 TCGA samples with post-bronchodilator pulmonary function were categorized into two groups: NSCLC with COPD ($n=65$) and NSCLC without COPD ($n=110$). Immunologic infiltration analysis through CYBERSORT algorithm based on the data showed that NSCLC with COPD exhibited an increased proportion of $CD8^+$T cells and a decreased proportion of Treg compared to NSCLC without COPD (Fig. 5A). Flow cytometry analysis was used further to compare the proportion and function of T cells and revealed a greater proportion of $CD8^+CD103^+$TRM within $CD3^+$T

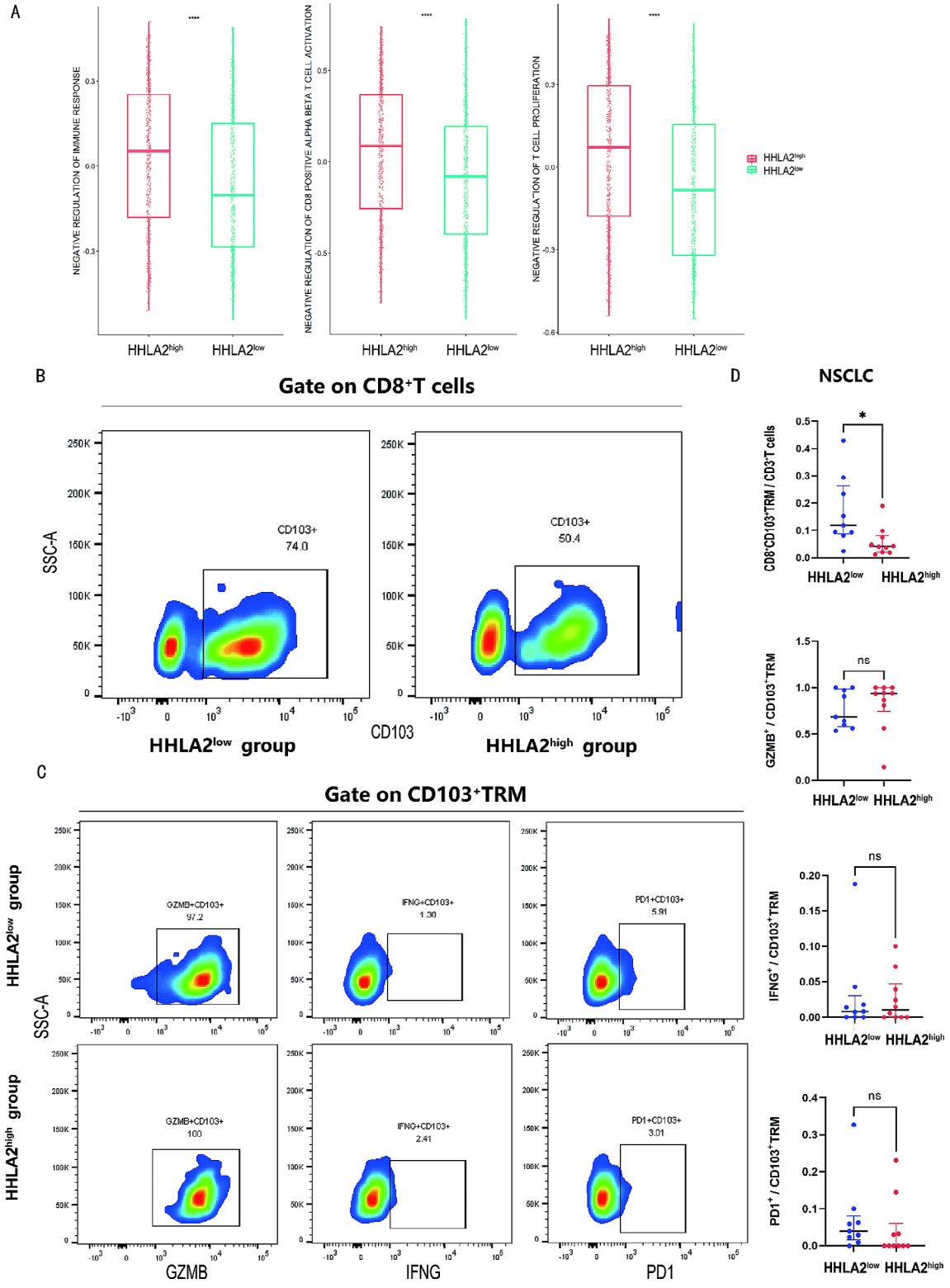

Fig. 3 Down-regulated HHLA2 was associated with $CD8^+CD103^+$TRM enrichment. (**A**) Comparison of negative regulation of immune response, T cell proliferation, and $CD8^+$T cell activation gene sets from the MSigDB database based on TCGA in the $HHLA2^{low}$ and $HHLA2^{high}$ group. (**B**) Representative flow cytometry chart of $CD8^+CD103^+$TRM in the $HHLA2^{low}$ versus $HHLA2^{high}$ group. (**C**) Representative flow cytometry chart of GZMB, IFNG, PD1 among $CD8^+CD103^+$TRM in the $HHLA2^{low}$ versus $HHLA2^{high}$ group. (**D**) Statistical maps of $CD8^+CD103^+$TRM proportion and function in the $HHLA2^{low}$ versus $HHLA2^{high}$ group. $^*P<0.05$, $^{**}P<0.01$, $^{***}P<0.001$, $^{****}P<0.0001$

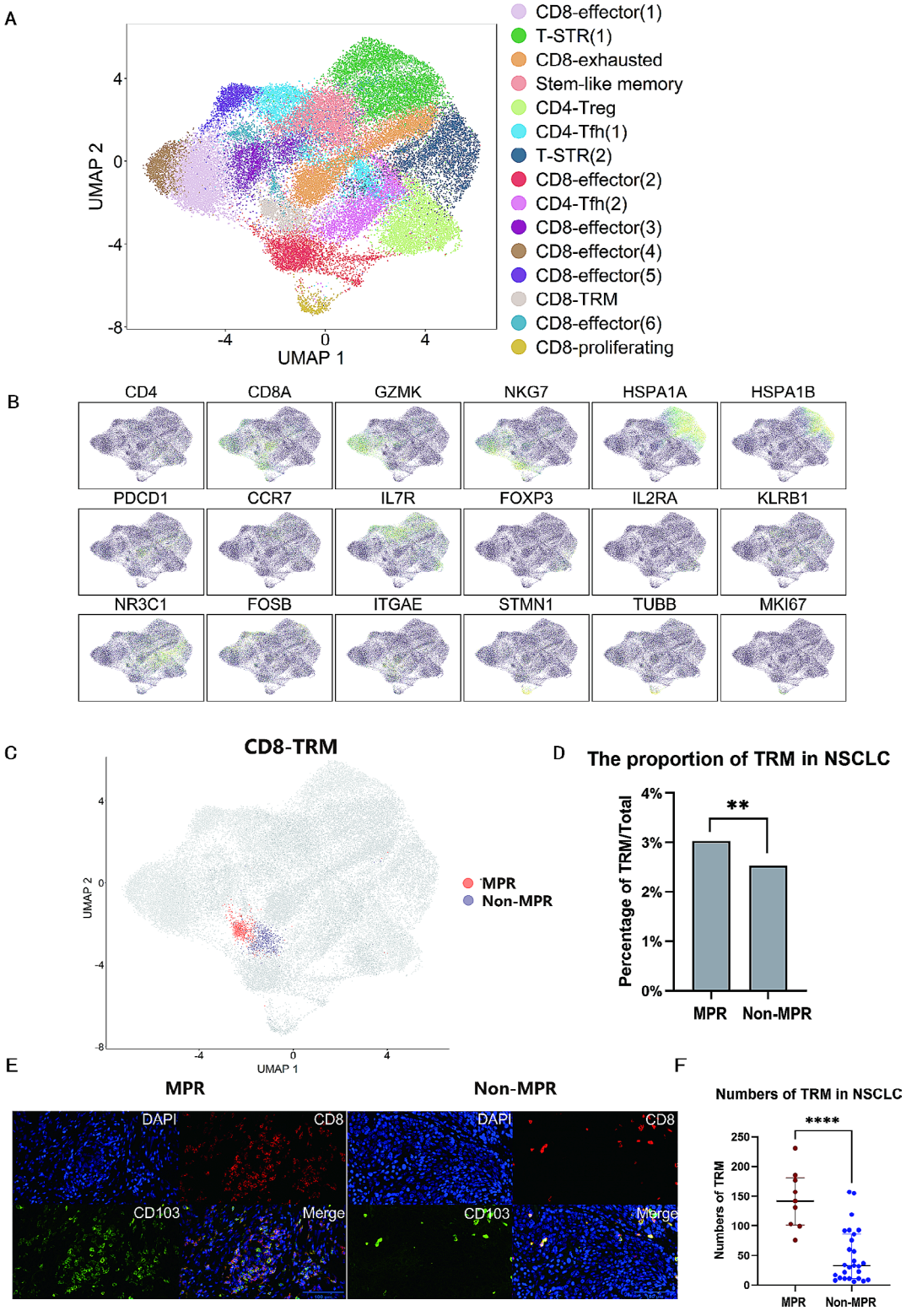

Fig. 4 The enrichment of $CD8^+CD103^+$TRM in the MPR group. (**A**) Single-cell analysis divided 42,678 cells into 15 sub-clusters. Treg, regulatory T cells; T-STR, stress response state T cells; Tfh, T follicular helper cells. (**B**) Expression of T cell subset-defining genes. (**C**) Distribution image of $CD8^+CD103^+$TRM in the MPR versus non-MPR group. (**D**) Statistical chart of the proportion of $CD8^+CD103^+$TRM in single-cell analysis in the MPR versus non-MPR group. (**E**) Representative images of TRM in immunofluorescence analysis. Left: the MPR group; Right: the non-MPR group. (**F**) Statistical chart of TRM of immunofluorescence analysis in the MPR versus non-MPR group. Scale bars, 100 μm. $^*P < 0.05$, $^{**}P < 0.01$, $^{***}P < 0.001$, $^{****}P < 0.0001$

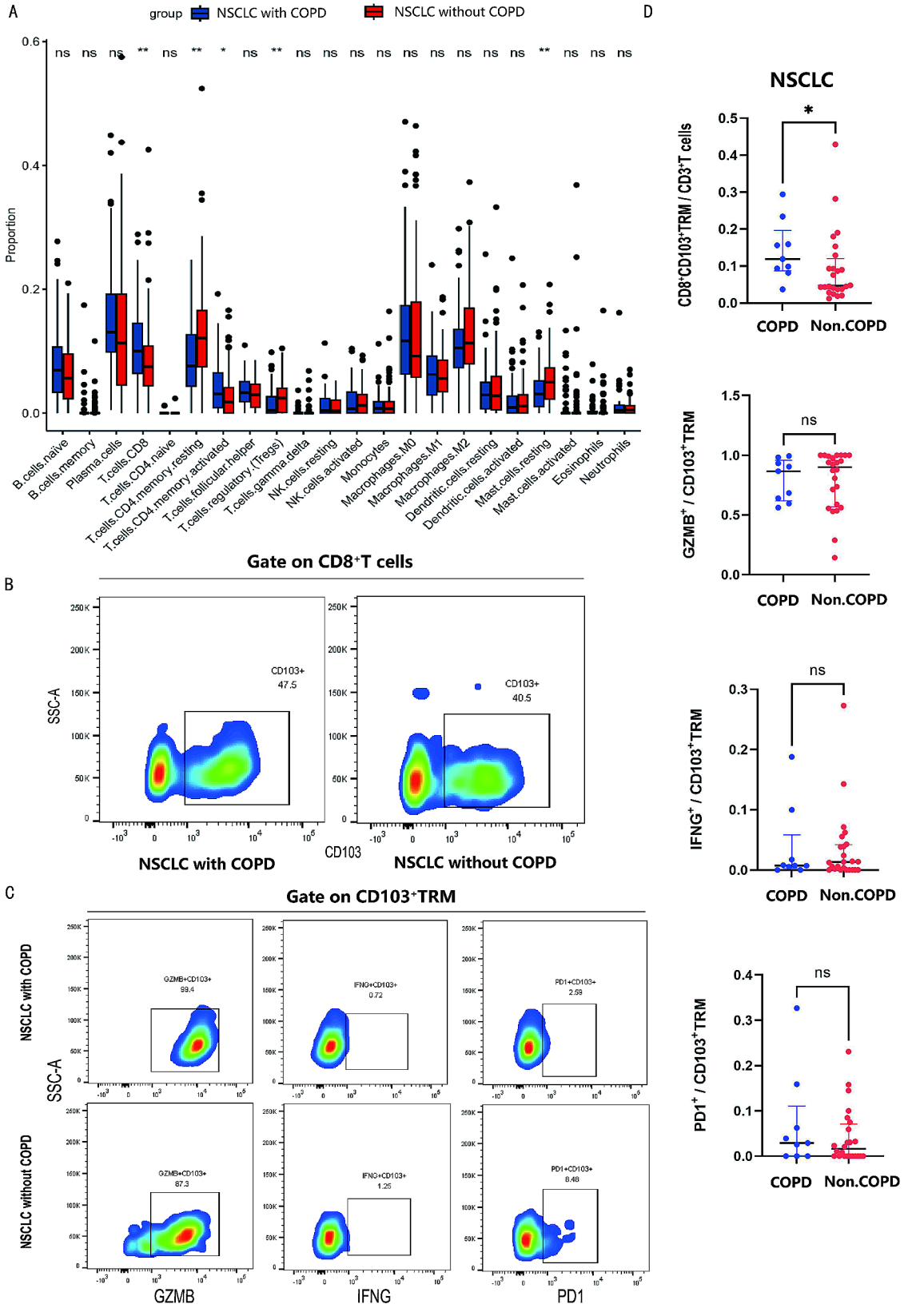

Fig. 5 NSCLC with COPD was featured by $CD8^+CD103^+$TRM enrichment. (**A**) Immune infiltration analysis in NSCLC with COPD versus NSCLC without COPD via CIBERSORT based on TCGA data. (**B**) Representative flow cytometry chart of $CD8^+CD103^+$TRM in NSCLC with COPD versus NSCLC without COPD. (**C**) Representative flow cytometry chart of GZMB, IFNG, PD1 among $CD8^+CD103^+$TRM in NSCLC with COPD versus NSCLC without COPD. (**D**) Statistical maps of $CD8^+CD103^+$TRM proportion and function in NSCLC with COPD versus NSCLC without COPD. $^*P < 0.05$, $^{**}P < 0.01$, $^{***}P < 0.001$, $^{****}P < 0.0001$

cells in NSCLC with COPD ($n=9$) compared to NSCLC without COPD ($n=24$) (11.9% vs. 4.6%, $P=0.040$). Nevertheless, there were no statistically significant differences among the expression of GZMB, IFNG, and PD1 among $CD8^+CD103^+$TRM cells between two groups (Fig. 5B-D). These outcomes validated that $CD8^+CD103^+$TRM were accumulated in NSCLC with COPD.

Discussion

This study was the first to identify NSCLC with COPD patients as an advantaged population for neoadjuvant immunotherapy. Down-regulated HHLA2 in NSCLC with COPD might improve the response to neoadjuvant immunotherapy by means of the enrichment of $CD8^+CD103^+$TRM.

Previous research have demonstrated that lung cancer patients with COPD had certain characteristics that suggested they may benefit from immunotherapy, such as high TMB, high tumor neo-antigen burden (TNB), high mutation frequencies of immune-related genes like LRP1B and PREX2, and low mutation frequency of EGFR [21, 22]. Furthermore, it has been reported that advanced NSCLC with COPD had a better overall survival (OS) and PFS compared to NSCLC without COPD when treated by immunotherapy [23]. Building upon these findings, our study further investigated the therapeutic effectiveness of neoadjuvant immunotherapy, demonstrating that NSCLC with COPD could obtain a better MPR rate than NSCLC without COPD.

The immune checkpoint expression profiles in the airway tissue of COPD showed the down-regulation of HHLA2 and lymphocyte activation gene-3 (LAG3), as well as the up-regulation of PD1 compared to health control [24]. Our study, through sequencing and immunohistochemical analysis, showed that NSCLC with COPD exhibited down-regulation of HHLA2 expression in the tumor immune microenvironment, particularly in tumor cells. HHLA2 was reported to disrupt anti-tumor immunity and inhibit immune surveillance [25]. In addition, Zhou et al. demonstrated that the co-expression of HHLA2 and PD-L1 negatively impacted the prognosis of clear cell renal cell carcinoma patients, suggesting these patients may derive advantages from the combined inhibition of both PD-L1 and HHLA2 [26]. Similar findings regarding the dual blockade of PD-L1 and HHLA2 have also been reported in spinal chordoma patients [27]. Our study further confirmed the down-regulation of HHLA2 in NSCLC patients achieving MPR.

Previous reports showed that HHLA2 initially inhibited T-cell proliferation and cytokine production by inhibiting phosphatidylinositol-3 kinases (PI3K)-protein kinase B (PKB/AKT) signaling [11, 28]. When HHLA2 was down-regulated, this inhibitory effect was weakened, thus promoting the anti-tumor immune system. Additionally, HHLA2/Killer Cell Immunoglobulin Like Receptor, Three Ig Domains And Long Cytoplasmic Tail 3 (KIR3DL3) signaling was reported to participate in modulating tissue-resident and innate-like T cells [29]. Our study confirmed that down-regulated HHLA2 was associated with $CD8^+CD103^+$TRM enrichment.

TRM were regarded as a foundation for effective neoadjuvant immunotherapy. These cells were believed to rapidly initiate the immune response against the tumor following treatment [30, 31]. In addition, previous research confirmed TRM infiltrating NSCLC tumors as activated cytotoxic cells, significantly contributing to anti-tumor immunity [17]. Similarly, when co-cultured with breast cancer cells, it was found that $CD8^+CD69^+CD103^+$TRM exhibited higher levels of IFNG and tumor necrosis factor-alpha (TNF-α) compared to $CD8^+CD69^+CD103^-$T cells, further mediating a more significant tumor-killing effect [32]. The augmentation of tumor-resident memory T cells correlated with improved survival outcomes in melanoma patients undergoing immunotherapy [33, 34]. In addition, TRM could convert “cold” into “hot” tumors, thereby improving the effectiveness of immunotherapy in gastrointestinal tumors [35]. Our study demonstrated the enrichment of TRM in the MPR group. This could be explained by the restoration of cytotoxic function in TRM following ICI therapy, thereby enhancing the efficacy of immunotherapy.

The potential advantages of neoadjuvant immunotherapy for NSCLC with COPD may be attributed to the long-term chronic inflammation and remodeling of the pulmonary immuno-microenvironment. The increased proportion of $CD8^+$T cells and T cell functional exhaustion were identified as critical immunophenotypic features in COPD [36–38]. Our study further validated the distribution of TRM in NSCLC with COPD versus NSCLC without COPD, and confirmed the enrichment of TRM in NSCLC with COPD.

Our study existed several limitations. First, the retrospective analysis of neoadjuvant immunotherapy’s effectiveness was hindered by patient bias towards LUSC, smoking history, and preference for combined immunotherapy and chemotherapy, complicating the differentiation between their respective efficacies and analysis based on smoking status. Second, due to the difficulty in obtaining NSCLC samples from patients who had concurrent COPD and underwent neoadjuvant immunotherapy, our study mainly utilized NSCLC surgical samples for analyses. Third, this study was lack of genomic information and the detailed mechanisms underlying the study results required further validation.

Conclusions

In summary, the study identified NSCLC with COPD patients as an advantaged population for neoadjuvant immunotherapy, offering a new perspective on the multimodality treatment of these patients. Down-regulated HHLA2 in NSCLC with COPD might improve the MPR rate to neoadjuvant immunotherapy by means of the enrichment of $CD8^+CD103^+$TRM.

Abbreviations

COPD	chronic obstructive pulmonary disease
NSCLC	non-small cell lung cancer
MPR	major pathologic response
OR	odds ratio
CI	confidence interval
HHLA2	HERV–H LTR-associating protein 2
TRM	tissue-resident memory T cells
ICI	immune checkpoint inhibitors
PD-L1	programmed cell death ligand 1
TMB	tumor mutational burden
MMR	mismatch repair
PD1	programmed cell death 1
PFS	progression-free survival
APC	antigen-presenting cells
FEV1	forced expiratory volume in one second
FVC	forced vital capacity
TCGA	The Cancer Genome Atlas
GEO	Gene Expression Omnibus
HRP	horseradish peroxidase
GZMB	granzyme B
IFNG	interferon gamma
IQR	interquartile Range
TNB	tumor neo-antigen burden
OS	overall survival
LAG3	lymphocyte activation gene-3
PI3K	phosphatidylinositol-3 kinases
PKB	protein kinase B
KIR3DL3	Killer Cell Immunoglobulin Like Receptor, Three Ig Domains And Long Cytoplasmic Tail 3
LUSC	lung squamous cell carcinoma
LUAD	lung adenocarcinoma
T-STR	stress response state T cells
Tfh	T follicular helper cells
Treg	regulatory T cells
TNF-α	tumor necrosis factor-alpha

Supplementary Information

The online version contains supplementary material available at https://doi.org/10.1186/s12885-024-12137-5.

Supplementary Material 1

Acknowledgements

Not applicable.

Author contributions

Ao Zeng: Formal analysis, Methodology, Software, Visualization, Writing– original draft; Yanze Yin: Formal analysis, Methodology, Writing– review & editing; Zhilong Xu: Data curation; Abudumijiti Abuduwayiti: Data curation; Fujun Yang: Resources; Mohammed Saud Shaik: Writing– review & editing; Chao Wang: Investigation; Keyi Chen: Supervision; Chao Wang: Validation; Xinyun Fang: Investigation; Jie Dai: Conceptualization, Funding acquisition, Project administration, Writing– review & editing. All authors read and approved the final manuscript.

Funding

This study is supported by the National Natural Science Foundation of China (Grant No. 82172848), and Shanghai Pulmonary Hospital Fund (fkzr2105 and fkyq1908).

Data availability

The datasets used and/or analysed during the current study are available from the corresponding author on reasonable request.

Declarations

Ethics approval and consent to participate

The study was approved by the responsible Ethics Committee of Shanghai pulmonary hospital (K23-228). Informed consent was obtained from all subjects and/or their legal guardian(s).

Consent for publication

Not applicable.

Competing interests

The authors declare that they have no competing interests.

Author details

[1]Department of Thoracic Surgery, Shanghai Pulmonary Hospital, School of Medicine, Tongji University, 200433 Shanghai, China
[2]School of Medicine, Tongji University, 200092 Shanghai, China

Received: 24 January 2024 / Accepted: 17 March 2024
Published online: 29 March 2024

References

1. Yi YS, Ban WH, Sohng KY. Effect of COPD on symptoms, quality of life and prognosis in patients with advanced non-small cell lung cancer. BMC Cancer. 2018;18(1):1053.
2. Zhai R, Yu X, Shafer A, Wain JC, Christiani DC. The impact of coexisting COPD on survival of patients with early-stage non-small cell lung cancer undergoing surgical resection. Chest. 2014;145(2):346–53.
3. Haslam A, Prasad V. Estimation of the percentage of US patients with Cancer who are eligible for and respond to checkpoint inhibitor immunotherapy drugs. JAMA Netw Open. 2019;2(5):e192535.
4. Sholl LM, Hirsch FR, Hwang D, Botling J, Lopez-Rios F, Bubendorf L, et al. The promises and challenges of Tumor Mutation Burden as an Immunotherapy Biomarker: a perspective from the International Association for the Study of Lung Cancer Pathology Committee. J Thorac Oncol. 2020;15(9):1409–24.
5. Zhou J, Chao Y, Yao D, Ding N, Li J, Gao L, et al. Impact of chronic obstructive pulmonary disease on immune checkpoint inhibitor efficacy in advanced lung cancer and the potential prognostic factors. Transl Lung Cancer Res. 2021;10(5):2148–62.
6. Noda Y, Shiroyama T, Masuhiro K, Amiya S, Enomoto T, Adachi Y, et al. Quantitative evaluation of emphysema for predicting immunotherapy response in patients with advanced non-small-cell lung cancer. Sci Rep. 2022;12(1):8881.
7. Takayama Y, Nakamura T, Fukushiro Y, Mishima S, Masuda K, Shoda H. Coexistence of Emphysema with non-small-cell Lung Cancer predicts the therapeutic efficacy of Immune Checkpoint inhibitors. Vivo. 2021;35(1):467–74.
8. Kerdidani D, Magkouta S, Chouvardas P, Karavana V, Glynos K, Roumelioti F, et al. Cigarette smoke-Induced Emphysema exhausts early cytotoxic CD8(+) T cell responses against nascent Lung Cancer cells. J Immunol. 2018;201(5):1558–69.
9. Zhao R, Chinai JM, Buhl S, Scandiuzzi L, Ray A, Jeon H, et al. HHLA2 is a member of the B7 family and inhibits human CD4 and CD8 T-cell function. Proc Natl Acad Sci U S A. 2013;110(24):9879–84.
10. Janakiram M, Chinai JM, Fineberg S, Fiser A, Montagna C, Medavarapu R, et al. Expression, clinical significance, and receptor identification of the newest B7 family Member HHLA2 protein. Clin Cancer Res. 2015;21(10):2359–66.
11. Li Y, Lv C, Yu Y, Wu B, Zhang Y, Lang Q et al. KIR3DL3-HHLA2 and TMIGD2-HHLA2 pathways: the dual role of HHLA2 in immune responses and its potential therapeutic approach for cancer immunotherapy. J Adv Res. 2022.

12. Wei Y, Ren X, Galbo PM Jr., Moerdler S, Wang H, Sica RA et al. KIR3DL3-HHLA2 is a human immunosuppressive pathway and a therapeutic target. Sci Immunol. 2021;6(61).
13. Rieder SA, Wang J, White N, Qadri A, Menard C, Stephens G, et al. B7-H7 (HHLA2) inhibits T-cell activation and proliferation in the presence of TCR and CD28 signaling. Cell Mol Immunol. 2021;18(6):1503–11.
14. Cheng H, Borczuk A, Janakiram M, Ren X, Lin J, Assal A, et al. Wide expression and significance of Alternative Immune Checkpoint molecules, B7x and HHLA2, in PD-L1-Negative human lung cancers. Clin Cancer Res. 2018;24(8):1954–64.
15. Okla K, Farber DL, Zou W. Tissue-resident memory T cells in tumor immunity and immunotherapy. J Exp Med. 2021;218(4).
16. Banchereau R, Chitre AS, Scherl A, Wu TD, Patil NS, de Almeida P et al. Intratumoral CD103 + CD8 + T cells predict response to PD-L1 blockade. J Immunother Cancer. 2021;9(4).
17. Corgnac S, Malenica I, Mezquita L, Auclin E, Voilin E, Kacher J, et al. CD103(+) CD8(+) T(RM) cells accumulate in tumors of Anti-PD-1-Responder Lung Cancer patients and are tumor-reactive lymphocytes enriched with Tc17. Cell Rep Med. 2020;1(7):100127.
18. Newman AM, Liu CL, Green MR, Gentles AJ, Feng W, Xu Y, et al. Robust enumeration of cell subsets from tissue expression profiles. Nat Methods. 2015;12(5):453–7.
19. Caushi JX, Zhang J, Ji Z, Vaghasia A, Zhang B, Hsiue EH, et al. Transcriptional programs of neoantigen-specific TIL in anti-PD-1-treated lung cancers. Nature. 2021;596(7870):126–32.
20. Chu Y, Dai E, Li Y, Han G, Pei G, Ingram DR, et al. Pan-cancer T cell atlas links a cellular stress response state to immunotherapy resistance. Nat Med. 2023;29(6):1550–62.
21. Ma H, Zhang Q, Zhao Y, Zhang Y, Zhang J, Chen G, et al. Molecular and clinicopathological characteristics of Lung Cancer Concomitant Chronic Obstructive Pulmonary Disease (COPD). Int J Chron Obstruct Pulmon Dis. 2022;17:1601–12.
22. Zhang Q, Feng X, Hu W, Li C, Sun D, Peng Z, et al. Chronic obstructive pulmonary disease alters the genetic landscape and tumor immune microenvironment in lung cancer patients. Front Oncol. 2023;13:1169874.
23. Shin SH, Park HY, Im Y, Jung HA, Sun JM, Ahn JS, et al. Improved treatment outcome of pembrolizumab in patients with nonsmall cell lung cancer and chronic obstructive pulmonary disease. Int J Cancer. 2019;145(9):2433–9.
24. Xu L, Li F, Jiang M, Li Z, Xu D, Jing J, et al. Immunosuppression by Inflammation-Stimulated Amplification of Myeloid-Derived Suppressor Cells and changes in expression of Immune Checkpoint HHLA2 in Chronic Obstructive Pulmonary Disease. Int J Chron Obstruct Pulmon Dis. 2023;18:139–53.
25. Su Q, Du J, Xiong X, Xie X, Wang L. B7-H7: a potential target for cancer immunotherapy. Int Immunopharmacol. 2023;121:110403.
26. Zhou QH, Li KW, Chen X, He HX, Peng SM, Peng SR et al. HHLA2 and PD-L1 co-expression predicts poor prognosis in patients with clear cell renal cell carcinoma. J Immunother Cancer. 2020;8(1).
27. Xia C, Huang W, Chen YL, Fu HB, Tang M, Zhang TL, et al. Coexpression of HHLA2 and PD-L1 on Tumor cells independently predicts the survival of spinal Chordoma patients. Front Immunol. 2021;12:797407.
28. Gaud G, Lesourne R, Love PE. Regulatory mechanisms in T cell receptor signalling. Nat Rev Immunol. 2018;18(8):485–97.
29. Palmer WH, Leaton LA, Campos Codo A, Crute B, Roest J, Zhu S, et al. Polymorphic KIR3DL3 expression modulates tissue-resident and innate-like T cells. Sci Immunol. 2023;8(84):eade5343.
30. Luoma AM, Suo S, Wang Y, Gunasti L, Porter CBM, Nabilsi N, et al. Tissue-resident memory and circulating T cells are early responders to pre-surgical cancer immunotherapy. Cell. 2022;185(16):2918–e3529.
31. Tissue-Resident Memory T. Cells underlie Neoadjuvant Immunotherapy Response. Cancer Discov. 2022;12(9):OF2.
32. Virassamy B, Caramia F, Savas P, Sant S, Wang J, Christo SN, et al. Intratumoral CD8(+) T cells with a tissue-resident memory phenotype mediate local immunity and immune checkpoint responses in breast cancer. Cancer Cell. 2023;41(3):585–601. e8.
33. Liang M, Wang X, Cai D, Guan W, Shen X. Tissue-resident memory T cells in gastrointestinal tumors: turning immune desert into immune oasis. Front Immunol. 2023;14:1119383.
34. Edwards J, Wilmott JS, Madore J, Gide TN, Quek C, Tasker A, et al. CD103(+) Tumor-Resident CD8(+) T Cells Are Associated with Improved Survival in Immunotherapy-Naive Melanoma patients and Expand significantly during Anti-PD-1 treatment. Clin Cancer Res. 2018;24(13):3036–45.
35. Abdeljaoued S, Arfa S, Kroemer M, Ben Khelil M, Vienot A, Heyd B et al. Tissue-resident memory T cells in gastrointestinal cancer immunology and immunotherapy: ready for prime time? J Immunother Cancer. 2022;10(4).
36. Biton J, Ouakrim H, Dechartres A, Alifano M, Mansuet-Lupo A, Si H, et al. Impaired tumor-infiltrating T cells in patients with chronic obstructive Pulmonary Disease Impact Lung Cancer response to PD-1 blockade. Am J Respir Crit Care Med. 2018;198(7):928–40.
37. Mark NM, Kargl J, Busch SE, Yang GHY, Metz HE, Zhang H, et al. Chronic obstructive Pulmonary Disease alters Immune Cell Composition and Immune checkpoint inhibitor efficacy in Non-small Cell Lung Cancer. Am J Respir Crit Care Med. 2018;197(3):325–36.
38. Corleis B, Cho JL, Gates SJ, Linder AH, Dickey A, Lisanti-Park AC, et al. Smoking and human immunodeficiency virus 1 infection promote Retention of CD8(+) T cells in the Airway Mucosa. Am J Respir Cell Mol Biol. 2021;65(5):513–20.

Publisher's Note